Pd−Promoted Ni−P Electroless Deposition on a Hydrogen-Bonded Molecular Surface of a Supramolecular Fibrous Template

Daisuke Ishii,[†] Taichi Nagashima,[‡] Mitsuru Udatsu,[†] Ren-De Sun,[§] Yuuichi Ishikawa,[§] Shinichi Kawasaki,[‡] Mitsuaki Yamada,[‡] Tomokazu Iyoda,[†] and Masaru Nakagawa*[,†]

Chemical Resources Laboratory, Tokyo Institute of Technology, R1-26, 4259 Nagatsuta, Midori-ku, Yokohama 226-8503, Japan, Advanced Material Business Promotion Department, Osaka Gas Co., Ltd., 6-19-9 Torishima, Konohana-ku, Osaka 554-0051, Japan, and Nanodevice Research Laboratory, KRI Inc., Kyoto Research Park 134, Chudoji-minami-machi, Shimogo-ku, Kyoto 600-8813, Japan

Received September 13, 2005. Revised Manuscript Received January 8, 2006

A nickel−phosphorus (Ni−P) hollow microfiber was obtained by simply immersing a recyclable hydrogen-bonded supramolecular fibrous template made of amphoteric azopyridine carboxylic acid in an HCl-acidic $PdCl_2$ aqueous solution and in a Ni−P electroless plating bath, followed by template removal in an alkaline aqueous solution. The Ni−P hollow microfiber had an inner pore diameter of 0.5 μm and a wall thickness of about 50 nm. The mechanism of the Pd-promoted Ni−P electroless deposition on the template surface was revealed by XPS analysis and TEM observation. Coordination of the $[PdCl_4]^{2-}$ species and its subsequent hydrolysis and condensation polymerization to a tubular Pd^{2+} nanosheet and formation of the Pd^0 nanoparticle as plating catalyst were brought about on the molecular surface of successive head-to-tail $COOH\cdots NC_5H_4$ hydrogen bonds, which comprised the supramolecular fibrous template. The hydrogen-bonded surface ordered at a molecular level leading to the tubular Pd^{2+} nanosheet played an important role in homogeneous Pd-promoted Ni−P electroless deposition and allowed us to fabricate a uniform Ni−P hollow microfiber.

Introduction

Organic, inorganic, and metallic hollow microfibers with a pore diameter of less than a micrometer have attracted much attention because of the prospects of their unique physical and chemical properties.[1−3] Template synthesis is widely accepted as a simple, high-throughput, and cost-effective method for preparing such hollow microfibers. An interior surface of porous alumina and polymer membranes[4] and channel array glass[5] along with an exterior surface of lipid-based cylindrical tubules and rodlike micelles,[6] bolaamphiphile assemblages,[7] biological tobacco mosaic virus,[8] organogelator fibrils,[9] carbon nanotubes,[10] and electrospun polymer fibers[11] have been utilized as reliable templates. The hollow microfibers composed of oxides (SiO_2,[12] TiO_2,[13] Fe_2O_3,[12b] V_2O_5[14]), sulfides (CdS, PbS),[12b] metals (Al,[15] Ni,[16] Cu,[17] Au,[13b,18] Ag,[18] Pt,[19] Pd[19c]), and organic conducting polymers (poly(pyrrole), poly(thiophene))[4c,20] are fabricated by the template synthesis through condensation polymeri-

* To whom correspondence should be addressed. E-mail: mnakagaw@res.titech.ac.jp.
[†] Tokyo Institute of Technology.
[‡] Osaka Gas Co., Ltd.
[§] KRI Inc.

(1) Hamilton, E. J. M.; Dolan, S. E.; Mann, C. M.; Coloijin, H. O.; McDonald, C. A.; Shore, S. G. *Science* **1993**, *260*, 659.
(2) Gleize, P.; Shouler, M. C.; Gadelle, P.; Gaillet, M. *J. Mater. Sci.* **1994**, *29*, 1575.
(3) Xia, Y.; Yang, P. *Adv. Mater.* **2003**, *15*, 351.
(4) (a) Martin, C. R. *Adv. Mater.* **1991**, *3*, 457. (b) Martin, C. R. *Acc. Chem. Res.* **1995**, *28*, 61. (c) Martin, C. R. *Science* **1994**, *266*, 1961. (d) Lakshimi, B. B.; Patrissi, C. J.; Martin, C. R. *Chem. Mater.* **1997**, *9*, 2544.
(5) Tonucci, R. J.; Justus, B. L.; Campillo, A. J.; Ford, C. E. *Science* **1992**, *258*, 783.
(6) (a) Schnur, J. M.; Price, R.; Schoen, P.; Yager, P.; Calvert, J. M.; Georger, J.; Singh, A. *Thin Solid Films* **1987**, *152*, 181. (b) Schnur, J. M. *Science* **1993**, *262*, 1669.
(7) Fuhrhop, J.-H.; Wang, T. *Chem. Rev.* **2004**, *104*, 2901.
(8) Douglas, T.; Young, M. *Adv. Mater.* **1999**, *18*, 679.
(9) (a) Mann, S.; Burkett, S. L.; Davis, S. A.; Fowler, C. E.; Mendelson, N. H.; Sims, S. D.; Walsh, D.; Whilton, N. T. *Chem. Mater.* **1997**, *9*, 2300. (b) Caruso, R. A.; Antonietti, M. *Chem. Mater.* **2001**, *13*, 3272.
(10) (a) Ajayan, P. M.; Vajtai, R. *NATO Sci. Ser., Ser. E* **2001**, *372*, 315. (b) van Bommel, K. J. C.; Friggeri, A.; Shinkai, S. *Angew. Chem., Int. Ed.* **2003**, *42*, 9870.
(11) Bognitzki, M.; Czado, W.; Frese, T.; Schaper, A.; Hellwig, M.; Steinhart, M.; Greiner, A.; Wendroff, J. H. *Adv. Mater.* **2001**, *13*, 70.
(12) (a) Ono, Y.; Nakashima, K.; Sano, M.; Kanekiyo, Y.; Inoue, K.; Hojo, J.; Shinkai, S. *Chem. Commun.* **1998**, 1477. (b) Shenton, W.; Douglas, T.; Young, M.; Stubbs, G.; Mann, S. *Adv. Mater.* **1999**, *11*, 253. (c) Miyaji, F.; Davis, S. A.; Charmant, J. P. H.; Mann, S. *Chem. Mater.* **1999**, *11*, 3021. (d) Harada, M.; Adachi, M. *Adv. Mater.* **2000**, *12*, 839. (e) Zhang, M.; Bando, Y.; Wada, K. *J. Mater. Res.* **2000**, *15*, 387. (f) Jung, J. H.; Shinkai, S.; Shimizu, T. *Nano Lett.* **2002**, *2*, 17.
(13) (a) Hoyer, P. *Langmuir* **1996**, *12*, 1411. (b) Hoyer, P. *Adv. Mater.* **1996**, *8*, 857. (c) Kasuga, T.; Hiramatsu, M.; Hoson, A.; Sekino, T.; Niihara, K. *Langmuir* **1998**, *14*, 3160. (d) Imai, H.; Takei, Y.; Shimizu, K.; Matsuda, M.; Hirashima, H. *J. Mater. Chem.* **1999**, *9*, 2971. (e) Kobayashi, S.; Hanabusa, K.; Hamasaki, N.; Kimura, M.; Shirai, H. *Chem. Mater.* **2000**, *12*, 1523.
(14) (a) Muhr, H.-J.; Krumeich, F.; Schonholzer, U. P.; Bieri, F.; Niederberger, M.; Gauckler, L. J.; Nesper, R. *Adv. Mater.* **2000**, *12*, 231. (b) Kobayashi, S.; Hamasaki, N.; Suzuki, M.; Kimura, M.; Shirai, H.; Hanabusa, K. *J. Am. Chem. Soc.* **2002**, *124*, 6550.
(15) Bognitzki, M.; Hou, H.; Ishaque, M.; Frese, T.; Hellwig, M.; Schwarte, C.; Schaper, A.; Wendorff, J. H.; Greiner, A. *Adv. Mater.* **2000**, *12*, 637.
(16) (a) Schnur, J. M.; Schoen, P. E.; Yager, P.; Calvert, J. M.; Georger, J. H.; Price, R. U.S. Patent 4911981, 1990. (b) Kong, F. Z.; Zhang, X. B.; Xiong, W. Q.; Liu, F.; Huang, W. Z.; Sun, Y. L.; Tu, J. P.; Chen, X. W. *Surf. Coat.* **2002**, *155*, 33. (c) Ang, L.-M.; Hor, T. S. A.; Xu, G.-Q.; Tung, C.-H.; Zhao, S.; Wang, J. L. S. *Chem. Mater.* **1999**, *11*, 2115. (d) Tai, Y.-L.; Teng, H. *Chem. Mater.* **2004**, *16*, 338.
(17) Browning, S. L.; Lodge, J.; Price, P. R.; Schelleng, J.; Schoen, P. E.; Zabetakis, D. *J. Appl. Phys.* **1998**, *84*, 6109.

10.1021/cm052050e CCC: $33.50
Published on Web 03/16/2006

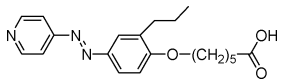

Figure 1. Chemical structure of an amphoteric azopyridine carboxylic acid forming a hydrogen-bonded fibrous molecular aggregate as a supramolecular template.

zation, electroless and electrochemical deposition, and physical and chemical vapor deposition.

Briefly, in the case of such an organic substance used as a template, the exterior surface is covered with oxide by condensation polymerization or with metal by electroless deposition, which results in the fabrication of inorganic−organic or metallic−organic hybrid microfibers. The outermost oxide or metal tubular material is obtained by template pyrolysis and by template extraction with an organic solvent. The template pyrolysis at a high temperature is suitable for the preparation of oxide hollow microfibers. An inert gas atmosphere is required for metallic hollow microfibers in order to avoid metal oxide formation. The template pyrolysis is an energy-consuming process, resulting in the emission of volatile organic substances and CO_2 from the organic template. In the latter case of template extraction, a flammable and unhealthy organic solvent is used, because such an organic template is generally soluble in organic solvents and insoluble in aqueous solutions suitable for electroless deposition and condensation polymerization. To achieve green sustainable chemistry, the industry standpoint is that a more-sophisticated fibrous organic template suitable for the preparation of metallic hollow microfibers without template pyrolysis and extraction with an organic solvent is desirable.

We have studied the self-assembled morphology[21] and template functionality[22] of hydrogen-bonded molecular aggregates formed from a series of amphoteric azopyridine carboxylic acids, which possess a basic pyridyl group as a hydrogen-bond acceptor and an acidic carboxyl group as a hydrogen-bond donor at their respective molecular terminals, as indicated in Figure 1. Self-assembly from their alkaline aqueous solution by neutralization allows us to prepare a fibrous hydrogen-bonded molecular aggregate with a submicrometer diameter. The emergence of the fibrous aggregate was due to the bundle formation of supramolecular polymers composed of successive intermolecular head-to-tail hydrogen bonds between pyridyl and carboxyl groups. The molecular long axis of the amphoteric molecule is aligned parallel to the long axis of the one-dimensionally growing fibrous molecular aggregate. Taking note of the molecular assembly and disassembly in aqueous solutions, we intended to use the fibrous molecular aggregate as an advanced recyclable supramolecular fibrous template available in environmentally friendly water media, as indicated in Figure 2. A Ni−P hollow microfiber was molded successfully from the supramolecular fibrous template by simple Ni−P electroless deposition using an acidic $PdCl_2$ aqueous solution. Moreover, the diameter and entire morphology of the supramolecular fibrous template could be varied by changing the kind of side-chain group to methyl, ethoxy, and *sec*-butyl groups, instead of the propyl group indicated in Figure 1. As a result, a variety of rod and helix Ni−P hollow microfibers were obtainable. The new supramolecular fibrous template has distinctive advantages of recycling and morphology-tuning ability. The initial study has been published as a communication.[22] During the study, we investigated whether the Ni−P hollow microfibers could be molded precisely from the fibrous hydrogen-bonded molecular aggregates. We therefore intended to investigate each chemical reaction in the electroless deposition in detail and reveal the mechanism of the Ni−P electroless deposition on a hydrogen-bonded molecular surface of the supramolecular fibrous template.

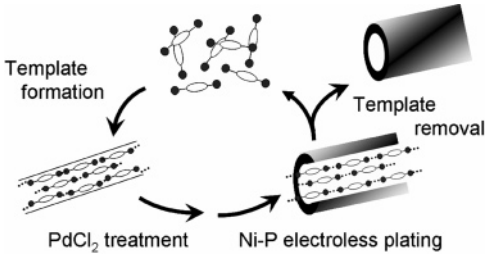

Figure 2. Illustration of a method for preparing Ni−P hollow microfibers using a recyclable hydrogen-bonded fibrous molecular aggregate. The method consists of template formation, $PdCl_2$ treatment, Ni−P electroless plating, and template removal.

In this article, we describe Pd-promoted Ni−P electroless deposition on the supramolecular fibrous template made of 6-[2-propyl-4-(4-pyridylazo)phenoxy]hexanoic acid. Surface adsorption of $[PdCl_4]^{2-}$ species on the hydrogen-bonded molecular surface and reduction of adsorbed Pd^{2+} species leading to Ni−P electroless deposition were investigated by X-ray photoelectron spectroscopy (XPS) and transmission electron microscopy (TEM). In addition, the detailed mechanism of forming the Ni−P hollow microfiber was described.

Experimental Section

Materials. 6-[2-Propyl-4-(4-pyridylazo)phenoxy]hexanoic acid was synthesized according to the procedure described in our previous paper.[21b] Palladium(II) chloride, disodium tetrachloropalladate, sodium hypophosphite monohydrate, nickel hypophosphite hexahydrate, boric acid, sodium acetate, ammonium sulfate, acetic acid, and sodium hydroxide were of reagent grade and were purchased from Kanto Kagaku, Japan. Distilled and deionized water was used for the preparation of Ni−P hollow microfibers. Deionized water of 18 MΩ cm after purification with a Millipore Mili-Q system was used for ICP-AES analysis.

Preparation of Ni−P Hollow Microfibers by Electroless Plating. 6-[2-Propyl-4-(4-pyridylazo)phenoxy]hexanoic acid (0.11 g, 0.31 mmol) was dissolved in an aqueous solution (300 mL) containing 3.0 mmol dm^{-3} NaOH. The orange transparent solution of pH 10.8 in a 500 mL glass beaker was stirred with a mechanical

(18) (a) Brumlik, C. J.; Menon, V. P.; Martin, C. R. *J. Mater. Res.* **1994**, *9*, 1174. (b) Satishkumar, B. C.; Vogl, E. M.; Govindaraji, A.; Rao, C. N. R.; *J. Phys. D* **1996**, *29*, 3173. (c) Demoustier-Champagne, S.; Delvaux, M. *Mater. Sci. Eng., C* **2001**, *15*, 269.
(19) (a) Liu, Z.; Lin, X.; Lee, J. Y.; Zhang, W.; Han, M.; Gan, L. M. *Langmuir* **2002**, *18*, 4054. (b) Mayers, B.; Jiang, X.; Sunderland, D.; Cattle, B.; Xia, Y. *J. Am. Chem. Soc.* **2003**, *125*, 13364. (c) Kijima, T.; Yoshimura, T.; Uota, M.; Ikeda, T.; Fujikawa, D.; Mouri, S.; Uoyama, S. *Angew. Chem., Int. Ed.* **2004**, *43*, 228.
(20) Goren, M.; Lennox, R. B. *Nano Lett.* **2001**, *1*, 735.
(21) (a) Aoki, K.; Nakagawa, M.; Ichimura, K. *Chem. Lett.* **1999**, 1205. (b) Aoki, K.; Nakagawa, M.; Ichimura, K. *J. Am. Chem. Soc.* **2000**, *122*, 10997. (c) Aoki, K.; Nakagawa, M.; Seki, T.; Ichimura, K. *Bull. Chem. Soc. Jpn.* **2002**, *75*, 2533.
(22) Nakagawa, M.; Ishii, D.; Aoki, K.; Seki, T.; Iyoda, T. *Adv. Mater.* **2005**, *17*, 200.

stirrer and kept standing for 3 days under an air atmosphere, giving a yellow suspension of pH 8 that contained a fibrous molecular aggregate. After being filtered and rinsed multiple times with distilled water, the fibrous aggregate was dispersed for 24 h in an acidic aqueous solution (300 mL, pH 2.5) containing 1.0 mmol dm^{-3} $PdCl_2$ and a small amount of concentrated HCl. The fibrous aggregate was filtered, washed with distilled water, and dispersed in a Ni−P electroless plating bath (500 mL, pH 5.5) containing 0.050 mol dm^{-3} $Ni(H_2PO_2)_2 \cdot 6H_2O$, 0.19 mol dm^{-3} H_3BO_3, 0.030 mol dm^{-3} CH_3COONa, and 9.8 mmol dm^{-3} $(NH_4)_2SO_4$ for 24 h at 25 °C. The plated fibrous molecular aggregate was filtered, washed with distilled water, and dispersed again in an alkaline aqueous solution (500 mL) of 1.0 mol dm^{-3} NaOH to dissolve the inner organic molecular aggregate as a center core. After stirring for 24 h, the Ni−P hollow microfiber was collected by filtration and rinsed with distilled water. The Ni−P hollow microfiber (0.56 g) was obtained after freeze drying. The pH values of aqueous solutions used in the Ni−P electroless plating were recorded on a Horiba B-212 pH meter.

Sample Characterization. SEM images of wet fibrous molecular aggregate were observed without metal coating using a Hitachi S-3000N SEM equipped with a cooling stage at −20 °C. SEM and TEM images of other samples were observed using a Hitachi S-800 field-emission SEM and a Hitachi H-7100 TEM. X-ray photoelectron spectra using Mg Kα radiation were measured by a Shimadzu ESCA3400 spectrometer. The radiation was not monochromated. The X-ray source was operated at 10 mA and 12 kV. The photoelectron takeoff angle was set at 90°. A binding energy scale was referenced to 285.0 eV, as was determined by the location of a maximum peak on the carbon 1s spectra of the hydrocarbon (CH). The accuracy of the binding energy was within 0.3 eV. The chemical compositions of the Ni−P hollow microfiber were characterized by ICP-AES using a Shimadzu ICP-8100 spectrometer. Freeze-dried Ni−P hollow microfiber was dissolved in a 1.0 mol dm^{-3} HNO_3 aqueous solution, and the resulting solution was analyzed by ICP-AES.

Results and Discussion

Template Synthesis of Ni−P Hollow Microfiber by Electroless Plating. Figure 3a indicates a SEM image of the supramolecular fibrous template made of 6-[2-propyl-4-(4-pyridylazo)phenoxy]hexanoic acid, with the result for its diameter distribution shown in the right column. The fibrous template possessed an average diameter of 552 nm and a length of 500−800 μm. Ni−P electroless plating on the fibrous template was carried out by its immersion in the HCl-acidic $PdCl_2$ aqueous solution and in the Ni−P electroless plating bath. Black-colored fibrous hybrid material was filtered and dispersed in an alkaline aqueous solution of 1.0 mmol dm^{-3} NaOH to remove the template. The Ni−P hollow microfiber was obtained after filtration and freeze drying. Panels b and c of Figure 3 show wide- and narrow-filed FE-SEM images of the Ni−P hollow microfiber. As can be seen, the Ni−P hollow microfiber had an inner diameter of about 500 nm and a length of several micrometers to several tens of micrometers. The ICP-AES analysis indicated that the Ni−P hollow microfiber was composed of 88% Ni, 11% P, and <2% Pd on the basis of weight. Approximately 1 wt % C was detected in the elemental analysis, indicating that the amphoteric molecule remained scarcely present. Two broad diffraction peaks centered at 45.0 and 80.0° in the powder XRD measurement suggested that deposited Ni−P alloy was in an amorphous phase.[22]

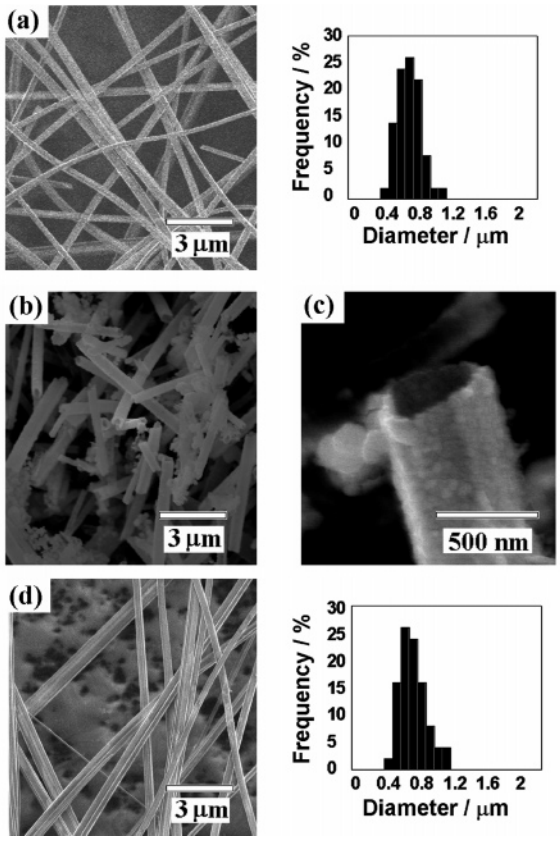

Figure 3. SEM images of fibrous molecular aggregates (a,d) and Ni−P hollow microfibers (b,c). The molecular aggregate images were taken (a) before the aggregate was used as a template and (d) after it was used as a template and reformed from an alkaline filtrate by HCl addition, with results for the diameter distribution shown in the right of panels a and d, respectively, of Figure 3. (b) Wide- and (c) narrow-field SEM images of the Ni−P hollow microfibers by the method shown in Figure 2.

The orange alkaline filtrate containing the template-forming molecule was acidified up to pH 5 by the addition of a concentrated HCl solution, and the resulting yellow powder was collected by filtration and observed by SEM. As can be seen in Figure 3d, the fibrous molecular aggregate with an average outer diameter of 563 nm was formed again. The collection yield of the fibrous molecular aggregate was 65%. It was found that the fibrous hydrogen-bonded molecular aggregate was available for a template to fabricate a Ni−P hollow microfiber by Ni−P electroless deposition. The fabrication process using the supramolecular fibrous template has two distinguishable advantages when compared with other organic templates such as lipid-based cylindrical tubules and organogelator fibrils. One advantage is that the Ni−P hollow microfiber could be prepared by extraction of the template-forming amphoteric molecule with an alkaline aqueous solution because of cleavage of the head-to-tail hydrogen bonds. Another advantage is that the supramolecular fibrous template was readily recyclable in environmentally benign water media because of reversible molecular assembly and disassembly, as illustrated in Figure 2.

Chemical Reactions in $PdCl_2$ Treatment. The inner diameter of the Ni−P hollow microfiber was molded from the outer diameter of the fibrous molecular aggregate, because Ni−P electroless deposition occurred uniformly on a molecular surface of the supramolecular fibrous template.

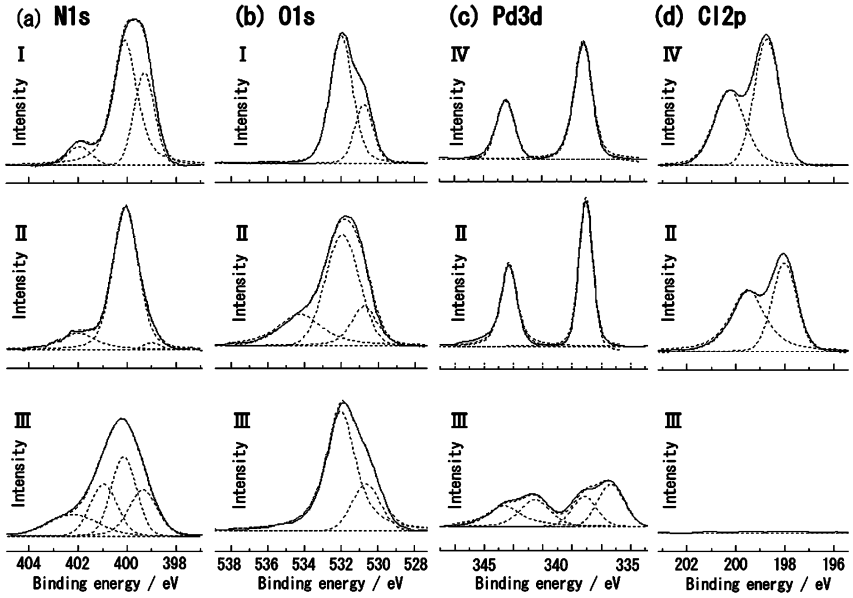

Figure 4. (a) Nitrogen 1s, (b) oxygen 1s, (c) palladium 3d, and (d) chlorine 2p XPS spectra of (I) the template (fibrous molecular aggregate), (II) $PdCl_2$-treated template, (III) NaH_2PO_2-treated template, and (IV) reference Na_2PdCl_4. Figure 4a-I means the N 1s spectrum observed for (I) the template, and so on.

Table 1. Core Electron Binding Energies (eV) Measured by XPS Spectra

	sample	N 1s	O 1s	Pd 3d	Cl 2p
I	template	399.3 (N···H), 400.1 (N═N), 401.9 (N^+−H)	530.8 (C−O−O^-), 532.0 (C−O, C═O)		
II	$PdCl_2$-treated template	399.0 (N···H), 400.1 (N═N, N−Pd), 402.0 (N^+−H)	530.9 (C−O−O^-), 532.0 (C−O, C═O), 534.2 (O−Pd)	338.1 ($Pd^{2+}{}_{5/2}$), 343.3 ($Pd^{2+}{}_{3/2}$)	198.0 (Pd−$Cl_{3/2}$), 199.5 (Pd−$Cl_{1/2}$)
III	$H_2PO_2^-$-treated template	399.3 (N···H), 400.1 (N═N, N−Pd), 401.0 (N−Pd), 402.0 (N^+−H)	530.8 (C−O−O^-), 532.0 (C−O, C═O)	336.3 ($Pd^0{}_{5/2}$), 338.2 ($Pd^{2+}{}_{5/2}$), 341.5 ($Pd^0{}_{3/2}$), 343.7 ($Pd^{2+}{}_{3/2}$)	
IV	Na_2PdCl_4 (ref)			338.2 ($Pd^{2+}{}_{5/2}$), 343.5 ($Pd^{2+}{}_{3/2}$)	198.7 (Pd−$Cl_{3/2}$), 200.2 (Pd−$Cl_{1/2}$)

The uniform Ni−P deposition layer was formed simply by immersion in the HCl-acidic $PdCl_2$ aqueous solution and then in the Ni−P electroless plating bath containing $H_2PO_2^-$ as reductant. We investigated whether the uniform Ni−P deposition layer was successfully formed on the molecular surface by the electroless deposition. We hereafter discuss what kind of chemical reaction occurred in the catalyzation with the $PdCl_2$ solution and the metallization with the plating bath by means of XPS and TEM.

$PdCl_2$ is dissolved as $[PdCl_4]^{2-}$ in a concentrated HCl aqueous solution. According to the report by Kind and coworkers,[23] it is anticipated that $[PdCl_4]^{2-}$ is the majority species and hydrolyzed $[PdCl_3(OH_2)]^-$ and $[PdCl_3(OH)]^{2-}$ are the minority species in the acidic $PdCl_2$ aqueous solution of pH 2.5 used in our study. Kuduk-Jaworska and coworkers[24] report that $K_2[PdCl_4]$ in an aqueous solution reacts with a pyridine derivative (Py) to give a complex $[PdCl_2(Py)_2]$. Taking account of the facts, we can deduce that $[PdCl_4]^{2-}$ reacted with a hydrogen-bonded pyridyl group located at an outermost surface of the fibrous molecular aggregate.

First of all, we measured two XPS spectra of the molecular aggregate before and after immersion in the HCl-acidic $PdCl_2$ aqueous solution, abbreviated as (I) template and (II) $PdCl_2$-treated template, to reveal the former catalyzation process. The nitrogen 1s, oxygen 1s, palladium 3d, and chlorine 2p XPS spectra are shown in Figure 4a−d, respectively. The deconvoluted peak electron binding energies are summarized in Table 1. As shown in Figure 4a-I, the N 1s spectrum of the (I) template could be fitted by two major components with peak binding energies (BEs) of 399.3 and 400.1 eV, which were attributable to nitrogen of a hydrogen bond (N···H)[25] and a diazo bond (N═N),[26] respectively. By the $PdCl_2$ treatment, the N 1s peak BE at 399.3 eV is lowered in intensity, as shown in Figure 4a-II. Instead, Pd $3d_{5/2}$ and Pd $3d_{3/2}$ BEs appeared at 338.1 and 343.3 eV (Figure 4c-II), and an O 1s BE appeared at 534.2 eV. The Cl $2p_{3/2}$ BE at 198.0 eV observed for (II) the $PdCl_2$-treated template (Figure 4d-II) was different from that at 198.7 eV observed for (IV) $Na_2[PdCl_4]$ as a reference (Figure 4d-IV).

Cis-$(C_5H_5N)_2PdCl_2$ gives a Pd $3d_{5/2}$ peak at 339.1 eV, and PdO gives a Pd $3d_{5/2}$ peak at 336.1 eV.[27] The observed $Pd_{5/2}$

(23) Kind, H.; Bittner, A. M.; Cavalleri, O.; Kern, K. *J. Phys. Chem. B* **1998**, *102*, 7582.
(24) Kuduk-Jawaorska, J.; Puszko, A.; Kubiak, M.; Pelczynska, M. *J. Inorg. Biochem.* **2004**, *98*, 1447.
(25) Wang, W. C.; Kang, E. T.; Neoh, K. G. *Appl. Surf. Sci.* **2002**, *199*, 52.
(26) Zhou, X. Q.; Li, L. W.; Chena, H. Z.; Wang, M. *Mater. Chem. Phys.* **1999**, *58*, 249.

BE at 338.1 eV was in the region observed for Pd^{2+} species,[28] indicating that Pd^{2+} was bound to nitrogen and/or chlorine.[23] Although the Pd $3d_{5/2}$ BE implied that the $[PdCl_4]^{2-}$ and $[PdCl_3(OH_2)]^-$ species in the acidic $PdCl_2$ solution reacted with the pyridyl group of the amphoteric molecule, we could not observed a new N 1s peak, indicating the formation of a Pd−N coordination bond in Figure 4a-II. An N 1s BE of the Pd−N bond might be overlapped with that of the diazo bond at 400.1 eV. To prove the overlap, we prepared a film of poly(4-vinyl pyridine-*co*-1-dodecyl-4-vinylpyridinium bromide)[29] on a silicon wafer and investigated XPS spectra of the film before and after its immersion in the acidic $PdCl_2$ solution. Before the immersion, the pyridyl and pyridinio moieties gave N 1s BEs at 399.1 and 401.6 eV, respectively. After the immersion, the BE of the pyridyl moiety was only shifted to 399.9 eV and a Pd $3d_{5/2}$ BE appeared at 338.1 eV (see the Supporting Information). Thus, we confirmed that the N 1s BE of a Pd−N bond at 399.9 eV was almost in agreement with that of the diazo bond (N═N) at 400.1 eV.

Taking account of the facts mentioned above, we can deduce the next: $[PdCl_4]^{2-}$ and $[PdCl_3(OH_2)]^-$ in the HCl-acidic $PdCl_2$ aqueous solution are reacted with a surface pyridyl group of the fibrous molecular aggregate by replacing chloride. Adsorbed Pd^{2+} species with a Pd $3d_{5/2}$ BE at 338.1 eV possess Pd−N, Pd−O, and/or Pd−Cl bonds, because the O 1s BE at 534.2 eV and the Cl $2p_{3/2}$ BE at 198.0 eV were observed for (II) the $PdCl_2$-treated template. As a result of the coordination of Pd^{2+} species, the surface hydrogen bond ($COOH\cdots NC_5H_4$) showing a N 1s BE at 399.3 eV is broken. The chemistry of Pd^{2+} halogen complexes in aqueous solution is dominant by hydrolysis above pH ~2[23,27,30] where hydroxo- and /or chloro-bridged Pd^{2+} oligomers[23,27,30] are formed by condensation.

TEM observation allowed us to prove the formation of such bridged Pd^{2+} oligomers on the template surface. The molecular aggregate after immersion in the $PdCl_2$ solution was dispersed in tetrahydrofuran (THF) to dissolve the template-forming amphoteric molecule. The resulting dark red solution was centrifuged, and the precipitate was dispersed in fresh THF again. A small amount of the THF solution was dropped on a carbon-coated Cu mesh, and the Cu mesh was dried and subjected to TEM observation. The result for the TEM observation is shown in Figure 5a. A lot of planular matter like a "cast-off shell of snake" with a width of about 500 nm was observed. Because the molecular aggregate was removed completely, the residual precipitate comes from surface-adsorbed Pd^{2+} species. The XPS and TEM results clearly showed the supramolecular fibrous template was covered entirely with tubular Pd^{2+}-nanosheet composed of well-condensed hydroxo- and chloro-bridged Pd^{2+} oligomers by its immersion in the HCl-acidic $PdCl_2$ aqueous solution.

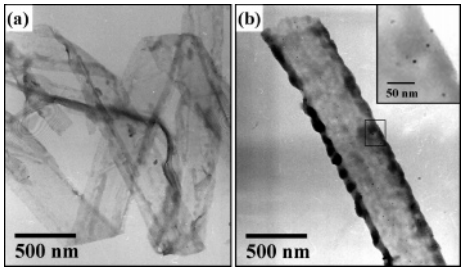

Figure 5. TEM images of (a) the $PdCl_2$-treated template and (b) the $H_2PO_2^-$-treated template after removal of the molecular aggregate with THF.

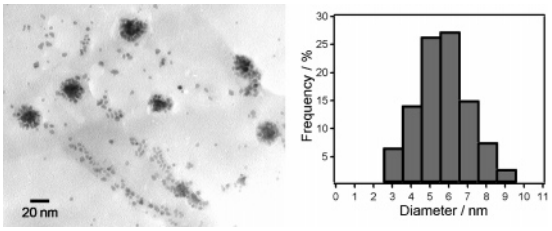

Figure 6. TEM image of Pd nanoparticles (left) in a supernatant prepared by centrifugation of a THF solution containing (III) $H_2PO_2^-$-treated template. (Right) the diameter distribution of the observed nanoparticles.

Chemical Reactions in the Ni−P Electroless Plating Bath Containing Reductant $H_2PO_2^-$. Pd^0 species reduced from Pd^{2+} species promotes the reduction of Ni^{2+} to Ni^0 in electroless plating, as reported by Alami and co-workers.[31] As described in the foregoing paragraph, the supramolecular fibrous template was covered with sheetlike Pd^{2+} species with a Pd $3d_{5/2}$ BE at 338.1 eV. Because the Pd^{2+} species cannot work as a catalyst to promote the reduction of Ni^{2+}, it was assumed that the Pd^{2+} species would be reduced in the Ni−P electroless plating bath. However, it was difficult to directly follow the formation of the Pd^0 species in the Ni−P plating bath, because a large amount of reduced Ni^0 species were generated simultaneously. We then prepared another plating bath containing 0.10 mol dm^{-3} NaH_2PO_2 as a reducing agent instead of 0.050 mol dm^{-3} $Ni(H_2PO_2)_2 \cdot 6H_2O$ in the Ni−P electroless plating bath and investigated the reduction of the sheetlike Pd^{2+} species by XPS and TEM.

The N 1s, Pd 3d, O 1s, and Cl 2p XPS spectra of the $PdCl_2$-treated molecular aggregate after immersion in the NaH_2PO_2 plating bath are shown in parts III of Figure 4a−d, respectively. The mark III means the sample of $PdCl_2$-treated molecular aggregate after immersion in the NaH_2PO_2 plating bath, which is abbreviated as (III) $H_2PO_2^-$-treated template hereafter. There were two features to note. Comparison of Figure 4b-III with Figure 4b-II clearly showed that new two Pd $3d_{5/2}$ and $3d_{3/2}$ BEs appeared at 336.3 and 341.5 eV, respectively. The Pd $3d_{5/2}$ BE at 336.3 eV obviously suggested that hydroxo- and/or chloro-bridged Pd^{2+} oligomers were reduced to Pd^0 species by $H_2PO_2^-$. No peak was observed for the Cl 2p spectra in Figure 4d-III. The NaH_2PO_2 plating bath exhibited a pH of 5.5. The disappearance of the Cl 2p BE and the existence of Pd^{2+} species with a Pd $3d_{5/2}$ BE of 338.2 eV indicated that hydroxo- and chloro-bridged Pd^{2+} oligomers were changed

(27) Dressick, W. J.; Dulcey, C. S.; Geoger, J. H., Jr.; Calabrese, G. S.; Calvert, J. M. *J. Electrochem. Soc.* **1994**, *141*, 210.
(28) Zhang, Y.; Tan, K. L.; Yang, G. H.; Kang, E. T.; Neoh, K. G. *J. Electrochem. Soc.* **2001**, *148*, C574.
(29) Suzuki, Y.; Nakagawa, M.; Iyoda, T. *Abstract No. 67*, 206th Meeting of The Electrochemical Society, Honolulu, HI, Oct 3−8, 2004; MA2004-02.
(30) Wyatt, I. R. *Chem. Weekbl.* **1966**, *62*, 10.
(31) Charbonnier, M.; Romand, M.; Harry, E.; Alami, M. *J. Appl. Electrochem.* **2001**, *31*, 57.

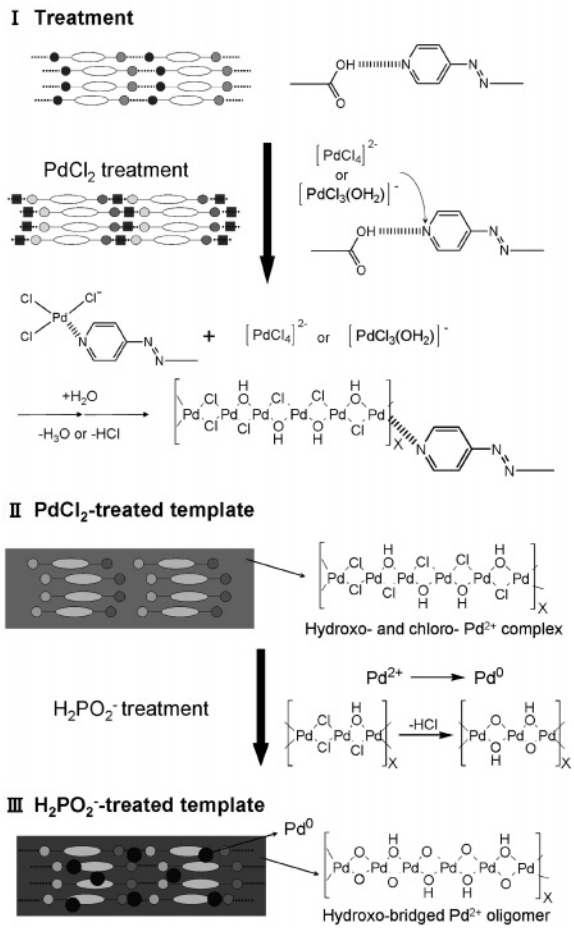

Figure 7. Schematic illustration of the formation of Pd^0 nanoparticles on the fibrous molecular aggregate by catalyzation with the acidic $PdCl_2$ aqueous solution and reduction with the NaH_2PO_2 aqueous solution.

to hydroxo-bridged Pd^{2+} oligomers by replacing chloride by hydroxide. This is in agreement with the chemistry of Pd^{2+} halogen complexes in aqueous solution that is dominant in hydrolysis above pH∼2.[23,27,30]

The template was removed from the (III) $H_2PO_2^-$-treated template by THF, and TEM observation on the residue was carried out. Figure 5b indicates the TEM image of the residues collected by centrifugation on a carbon-coated Cu mesh. A hollow fiber with dark dots was observed. It can be deduced from the XPS spectra that the hollow fiber was composed of hydroxo-bridged Pd^{2+} oligomers, and the dark dots were assigned to Pd^0 nanoparticles. When the supernatant separated by centrifugation was observed by TEM, a lot of Pd^0 nanoparticles could be visualized. The left of Figure 6 shows the TEM images of Pd^0 nanoparticles in the supernatant, with the result for their size distribution shown in the right of Figure 6. The Pd^0 nanoparticles had a size of 3−9 nm and an average diameter of 5.6 nm. The Pd^0 nanoparticles worked as catalysts to reduce Ni^{2+} to Ni^0 by the reductant $H_2PO_2^-$ in the Ni−P electroless plating bath.

Figure 7 illustrates the summarized mechanism for forming Pd^0 nanoparticle catalysts on the hydrogen-bonded molecular surface of the supramolecular fibrous template. First, $[PdCl_4]^{2-}$ of the majority species in the HCl-acidic $PdCl_2$ aqueous solution attacks the intermolecular head-to-tail hydrogen bond between the pyridyl and carboxyl groups, forming a Pd−N coordination bond by replacing a chloride of $[PdCl_4]^{2-}$ with the pyridyl group. Because the acidic $PdCl_2$ solution exhibits pH 2.5, the Pd^{2+} chlorine complex is hydrolyzed to hydroxo- and chloro-Pd^{2+} complexes, which were gradually condensed to hydroxo- and/or chloro-bridged Pd^{2+} oligomers. As a result, the supramolecular fibrous template is entirely covered with a tubular Pd^{2+} nanosheet. In the reduction by $H_2PO_2^-$, Pd^0 nanoparticles with the catalytic ability of Ni−P electroless deposition are formed from the nanosheet.

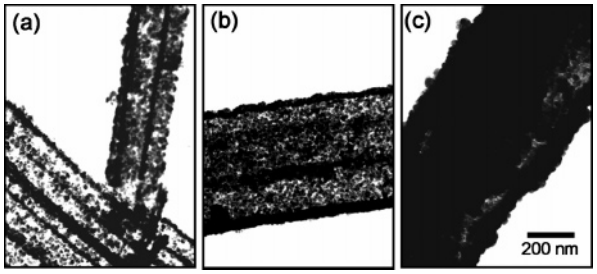

Figure 8. TEM images of a Ni−P hollow microfiber prepared in a Ni−P electroless plating bath of (a) 200, (b) 500, and (c) 1000 mL.

Control of Wall Thickness in a Ni−P Hollow Microfiber. Ni−P hollow microfibers in panels b and c of Figure 3 could be successfully obtained by immersing the $PdCl_2$-treated molecular aggregate in 500 mL of the Ni−P electroless plating bath containing $H_2PO_2^-$ as reductant, followed by removal of the molecular aggregate as a template with a 1 mol dm^{-3} NaOH aqueous solution. Figure 8b shows the TEM image of the Ni−P hollow microfiber. It was found that the Ni−P hollow microfiber had a wall thickness of 30−70 nm and was composed of Ni−P nanoparticles 10−20 nm in diameter.

To control the wall thickness in the Ni−P hollow microfiber, we carried out electroless plating using different amounts of the Ni−P electroless plating bath, 200, 500, and 1000 mL. The respective amounts correspond to the supramolecular fibrous template formed from 0.1 g of the amphoteric molecule. When the plating bath of 200 mL was used, a large amount of Ni−P grains and a small amount of irregular hollow microfibers were obtained. As can be seen in Figure 8a indicating the TEM image, there were a lot of defects in the wall due to incomplete coating by with Ni−P deposition. In contrast, when the 1000 mL plating bath was used, it was difficult to extract an inner template with the NaOH alkaline aqueous solution. As confirmed by Figure 8c, a hollow structure was barely observed. The supramolecular template still remained. From the edge of the Ni−P wall in Figure 8c, we estimated the thickness of the Ni−P wall to be more than 100 nm. It was found that the amphoteric molecule could not be extracted with the alkaline aqueous solution when the wall thickness was more than 100 nm. The length of the Ni−P hollow microfiber prepared from the plating bath of 500 mL was shorter (Figure 3b) than that of the fibrous template (Figure 3a). This shortening is due to snapping the plated fibrous template during template removal by stirring and filtration. The wall thickness of 30−70 nm was probably mechanically moderate in snapping the plated fibrous template and in maintaining the Ni−P hollow structure.

Conclusion

We found that Ni−P hollow microfibers were successfully molded from the hydrogen-bonded supramolecular fibrous template by Ni−P electroless deposition using a HCl-acidic $PdCl_2$ aqueous solution. Hydrolysis and condensation polymerization of Pd^{2+} chlorine complexes adsorbed on the hydrogen-bonded molecular surface by coordination gave a tubular Pd^{2+} nanosheet that entirely covered the template fibers. Pd^0 nanoparticles were formed by reduction of the nanosheet that could work as catalysts to promote Ni−P electroless deposition. The molecular surface that possessed intermolecular head-to-tail hydrogen bonds ($COOH\cdots NC_5H_4$) periodically at a molecular level was suitable for homogeneous condensation to form polymetalloxane bonds, leading to uniform Ni−P electroless deposition. A Ni−P amorphous phase can be transformed to fcc Ni and Ni_3P crystalline phases by annealing under an inert gas atmosphere.[16d] A Ni−P hollow microfiber containing a magnetic and conductive fcc Ni phase is promising for use as a lightweight conductive filler with orientational controllability under a commonly accessible magnetic field. The magnetic property and the orientational controllability in a polymer matrix will be published elsewhere.

Acknowledgment. This work was supported by the Industrial Technology Research Grant Program in 2005 (05A25011d) from the New Energy and Industrial Technology Development Organization (NEDO) of Japan.

Supporting Information Available: Diagram and XPS spectra of poly(4-vinyl pyridine-co-1-dodecyl-4-vinylpyridinium bromide) before and after its immersion the an acidic $PdCl_2$ solution (pdf). This material is available free of charge via the Internet at http://pubs.acs.org.

CM052050E